Long-range Doppler lidar measurements of wind turbine wakes and their interaction with turbulent atmospheric boundary-layer flow at Perdigao 2017

Long-range Doppler lidar measurements of wind turbine wakes and their interaction with turbulent atmospheric boundary-layer flow at Perdigão 2017

Norman Wildmann[1], Thomas Gerz[1], Julie K. Lundquist[2,3]

[1]Institute of Atmospheric Physics, Deutsches Zentrum für Luft- und Raumfahrt e.V., Oberpfaffenhofen, Germany.
[2]Department of Atmospheric and Oceanic Sciences, University of Colorado Boulder, Boulder, Colorado, USA
[3]National Renewable Energy Laboratory, Golden, Colorado, USA

E-mail: norman.wildmann@dlr.de

Abstract. As part of the Perdigão 2017 campaign, vertical RHI (range-height indicator) scans with long-range pulsed Doppler wind lidars were performed aligned with the main wind direction and a wind turbine (WT) located on a mountain ridge. The measurements are used to not only retrieve flow velocities, but also their variance and - by using the turbulent broadening of the Doppler spectrum - also turbulent kinetic energy (TKE) dissipation rate. The study shows that turbulence in the WT wake is dependent on the turbulence of the inflow, but also on atmospheric stability. In stable atmospheric conditions, wakes could be analyzed up to five rotor diameters downstream (D) and showed the maximum turbulence in the wake at 2-3 D, whereas in unstable conditions, the maximum was found at 2 D and the wake could not be detected further than 3 D. A clear dependency of wake turbulence enhancement on inflow turbulence intensity is found, which levels out to no further enhancement at turbulence intensities of 30%.

1. Introduction

Amongst the challenges in wind-energy research, turbulence plays an important role for the understanding of inflow conditions [1, 2]. Turbulence generated by wind turbines (WT) in their wakes is a feature that is inherent to every wind park and thus deserves special regards. Wakes, and their interaction with atmospheric flows, have been studied theoretically [3], in simulations [4, 5, 6, 7], and in experiments [8, 9, 10, 11, 12, 13]. With developments in measurement technology and analysis methods, more details of wind turbine wakes can be revealed through field experiments. The development of lidar technology had a large impact in the field. Short-range, continuous-wave Doppler wind lidars can provide very detailed measurements of the wake in the near-field of the turbine [14, 15]. Long-range pulsed Doppler wind lidars have been used in many studies to study the wake propagation in the far field [9, 16, 17]. In this study, we use long-range

lidars to measure turbulence parameters, i.e. velocity variance and turbulence kinetic energy dissipation rate from RHI (range-height indicator) scans. The measurements for this purpose were collected at the Perdigão 2017 experiment, which will be introduced in Sect. 2. Previous studies about the WT wake at Perdigão focussed on its propagation and wind speed deficit [18, 19, 20, 17, 21]. The method to retrieve turbulence in this study is presented in Sect. 3, followed by the results in Sect. 4 and the Conclusions.

2. Experiment and dataset

2.1. Perdigão 2017

The Perdigão 2017 experiment was carried out in central Portugal, close to the Spanish border at a location that is unique due to its nearly parallel mountain ridges in a distance of approximately 1.4 km to each other (see Fig. 1). Fernando et al. (2018) [22] gives an overview of all institutions that contributed to the campaign and their research goals as well as all the instrumentation that was deployed in the field. On the south-west (SW) ridge, a WT of type Enercon E-82 with a hub height of 78 m and a rotor diameter of 82 m is installed. The focus of the DLR participation was on interaction of the WT wake with the complex atmospheric flows in this terrain. For this purpose, three Doppler wind lidars of type Leosphere Windcube 200S were set up during the intensive operation period (IOP) from 01 May 2017 through 15 June 2017. More details on the DLR instrumentation can be found in [20, 17, 23]. In this study, data from lidar #2 are used which was installed in the Vale do Cobrão between the two mountain ridges, scanning up to the wind turbine. This lidar provided the best availability of wind turbine wake measurements.

2.2. Dataset

Within the IOP period, the lidar data were filtered for the following criteria:

- Wind direction between 225° and 245°.
- Wind speed between 5 m s^{-1} and 9 m s^{-1}.
- Wind turbine was operating.
- A wake signature could be detected in the RHI scan.
- Lidar was operational and collecting good data (CNR>-25dB).

The result of this filtering yields 40 hours of data. The data were then subdivided into nighttime cases with statically stable stratification (potential temperature gradient $\frac{\Delta\theta}{\Delta z} > 0$ and time of day between 20:00 UTC and 8:00 UTC) and daytime cases (all other cases). $\frac{\Delta\theta}{\Delta z}$ is calculated as an average in the lowest 300 m as measured by the microwave radiometer southwest of the Perdigão mountains (see [17]). The result is 6 hours of data in a stable atmosphere and 34 hours in neutral and unstable conditions. For further analysis, an averaging time of 30 minutes is used so that the number of analyzed time periods is twice the number of hours. The raw lidar data can be found in the Perdigão

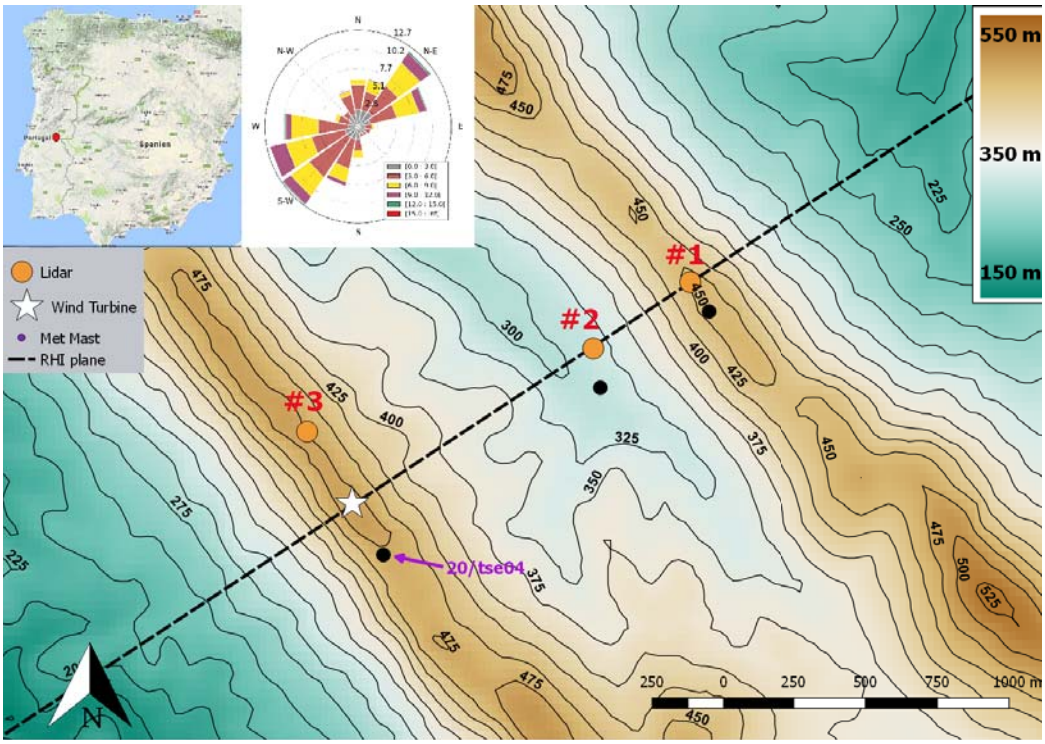

Figure 1. Map of the Perdigão map, indicating the location of DLR-operated scanning lidars, the 100 m meteorological masts and the wind turbine. The wind rose is showing wind measurements of the sonic at WT hub height on tower 20/tse04 during the IOP.

field experiment data repository [24].
High resolution measurements of the sonic anemometer at WT hub height (78 m) are used for comparison during the time periods of interest. The data can be found in the UCAR repository [25].

3. Methodology

3.1. Estimation of wake characteristics

Wildmann et al. (2018) [17] showed how coplanar RHI scans can be used to automatically detect the wake center and wind speed deficit within. For this study, we only analyze single lidar RHI scans from lidar #2 in the Vale do Cobrão. For the best availability of wake measurements, the automatic detection of wakes was quality controlled and enhanced by manual inspection of each half-hour averaged field of radial velocities. Along the detected wake paths, boxes of 20 m are defined within which the turbulence retrieval according to Wildmann et al. (2019) [23] was applied (see Fig. 2). A maximum distance of 400 m (i.e. five rotor diameters) was chosen, because few wakes were detected at larger distances.
The method uses the variance of line-of-sight velocities $\hat{\sigma}_v^2$ as a space and time average ($\Delta t = 1800\ s$) and the turbulent broadening of the Doppler spectrum σ_t^2 to obtain the

variance over all scales of the flow in lidar beam direction σ_v^2:

$$\sigma_v^2 = \hat{\sigma}_v^2 + \sigma_t^2 \tag{1}$$

To obtain the turbulent broadening σ_t^2, shear ($\hat{\sigma}_s^2$) and the spectral width at constant wind speed (σ_0^2) are removed from the spectral width ($\hat{\sigma}_{sw}^2$) as in [26]:

$$\sigma_t^2 = \hat{\sigma}_{\mathrm{sw}}^2 - \sigma_0^2 - \hat{\sigma}_s^2 \quad . \tag{2}$$

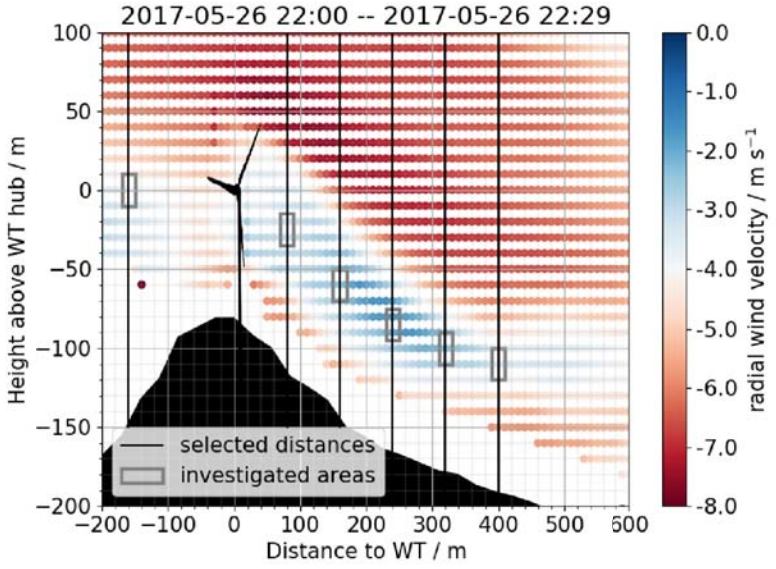

Figure 2. Example of a full RHI scan with indication of distances and areas of wake turbulence retrieval.

For turbulence that can be described with the von Kármán spectrum, and integral length scales larger than the lidar sensing volume, the integral length scale L_v and TKE dissipation rate ε can be retrieved from σ_t^2 and σ_v^2:

$$L_v = c_1 \left(\frac{\sigma_t^2}{\sigma_v^2} \right)^{c_2} + c_3 \tag{3}$$

$$\varepsilon = \frac{1.972}{C_k^{3/2}} \frac{\sigma_v^3}{L_v} \tag{4}$$

c_1, c_2 and c_3 are coefficients that are determined as an approximation of the full theory (for full derivation, see [23]) and $C_k = 2$ is used as the Kolmogorov constant. All values of ε are filtered where the calculated uncertainty of the method as in [23] is more than twice the actual value of ε. For this reason, the number of data points for ε is smaller than the number of measurements for velocity variance (only 35 half-hour periods in 1-2 rotor diameters downstream).

3.2. Estimation of background wind speed and turbulence

Analyzing wind speeds and turbulence in the wake raises the problem of an appropriate reference point (sometimes referred to as u_∞). The definition of u_∞ is particularly challenging for the Perdigão campaign as the inflow is forced upon a slope towards the SW ridge where the WT is located. We identified two possibilities to define the incoming flow. First, wind speed and variance can be determined from the lidar RHI scans at two rotor diameters upstream (see Fig. 2). Second, the sonic anemometer at hub height on the 100 m mast 20/tse04 can be used. While the lidar measurement upstream can be distorted by inclination of the flow over the slope, the tower sonic is displaced by approximately 200 m laterally and the flow at this point has a slightly different fetch than the flow hitting the WT. For scaling of the lidar measurements in this study we will use the lidar measurements two rotor diameters upstream, as in this case the systematic errors of the instrument and the method are the same as for the measurements in the wake and thus a better relative accuracy between wake and upstream measurements can be expected. The tower measurements will be displayed as a comparison. TKE dissipation rates from the sonic anemometers are estimated from a fit to the second order structure function as described in [27, 23].

4. Results

4.1. Wake turbulence in dependency of distance to the WT

Figure 3 shows the results of averaged wake variance in comparison to upstream flow variance. Figure 3a gives the absolute values, whereas Fig. 3b shows the results scaled to the incoming flow variance. From the absolute values we see that flow variance in the stable atmosphere is much lower than in other cases, which is particularly obvious in the upstream measurements as expected. It also shows that adding the turbulent broadening of the Doppler spectrum to the lidar measured variance increases the measured variance significantly by 20% in unstable conditions and up to 50% in stable conditions. In unstable conditions, no wake detection further than two rotor diameters D downstream could be clearly detected, while in stable conditions a detection up to 5 D was possible. A maximum of turbulence is detected at 2 D.

Looking at the ε-retrievals from the lidar measurements (Fig. 4), the findings from the variance analysis are confirmed. While the absolute values of ε as well as for σ_v^2 are not larger for the stable cases, the relative increase of turbulence is significantly larger, since the upstream turbulence is much lower. We know from previous studies that the lidar retrieval of ε is highly uncertain in stable regimes with low turbulence as in the upstream cases during the night in this study. Therefore the enhancement of ε is also subject to large uncertainties, especially since tower 20/tse04 shows a larger mean value of ε than the lidar upstream measurements.

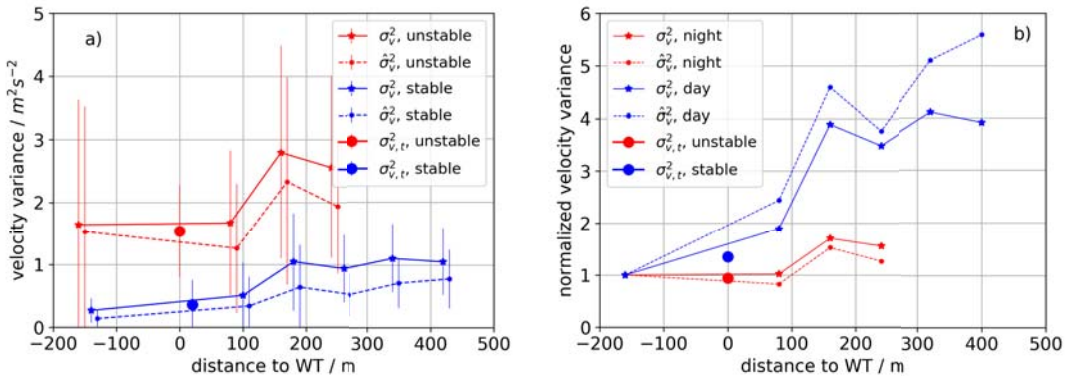

Figure 3. Measurements of flow averaged velocity variance σ_v^2 (solid lines) and $\hat{\sigma}_v^2$ (dashed lines) as a function of the distance to the wind turbine as measured by the lidar (a) and normalized by the incoming flow variance (b). Red depicts unstable conditions and blue stable conditions. Heavy markers at 0 distance to the WT are for corresponding tower 20/tse04 measurements. The error bars give the standard deviation of all half-hour averages. The measurement points of the individual curves in a) are successively shifted by 10 m (20 m, 30 m) from their original value for better readability of the error bars.

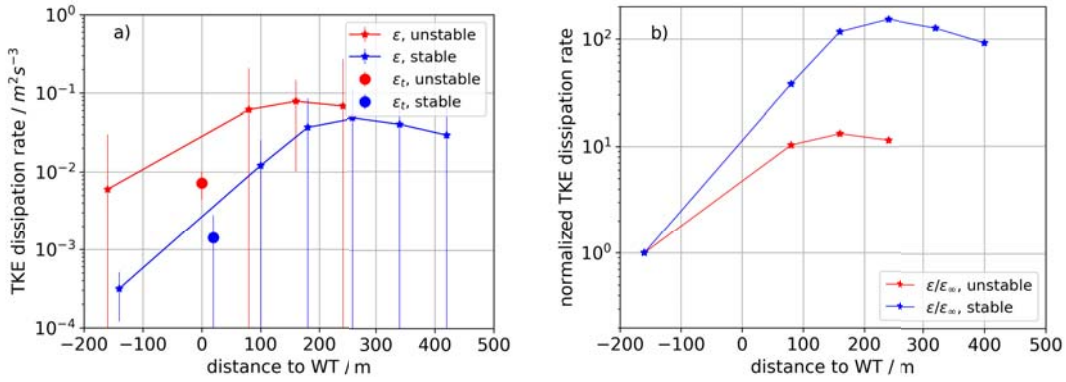

Figure 4. Measurements of flow averaged TKE dissipation rate ε as a function of the distance to the wind turbine as measured by the lidar (a) and scaled to the incoming flow ε (b). Red depicts unstable conditions and blue stable conditions. In (a), the error bars give the standard deviation of all half-hour averages. The measurement points are shifted by 10 m from their original value for better readability of the error bars. Heavy markers at 0 distance to the WT are for corresponding tower 20/tse04 measurements.

4.2. Evaluation of the dependency of wake characteristics on background turbulence

Instead of subdividing the data in stable and unstable cases only, we can also look at the overall relation of wake turbulence intensity $TI = \sigma_u/u$ to upstream turbulence intensity TI_∞ (Fig. 5). The increase in turbulence in the wake is related to upstream turbulence intensity. The absolute values of wake TI are in general higher than at the upstream location, but do not show a clear trend. Looking at the enhancement of turbulence

intensity TI/TI_∞ (Fig. 5) a decay of TI enhancement with upstream TI is detected. The scatter in the data reflects the uncertainty of the estimation of turbulence and the complexity of the flow at the Perdigão location.

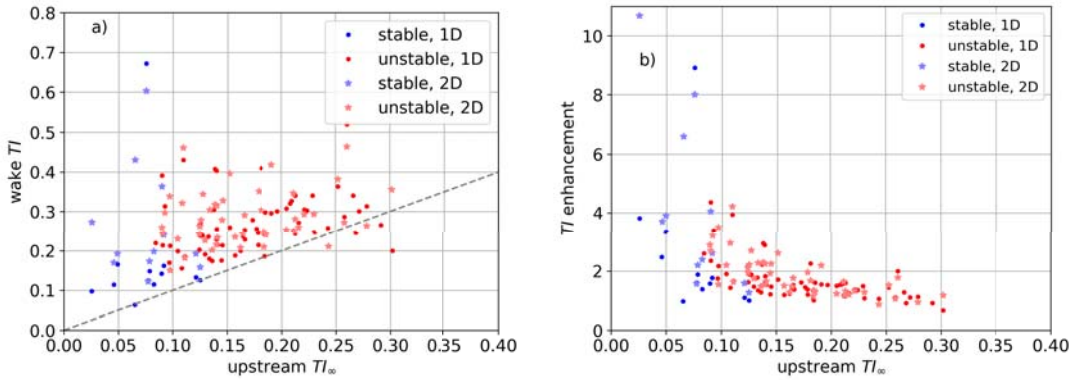

Figure 5. Turbulence intensity (TI) in the wake as a function of upstream turbulence (TI_∞) for distances of 1 D (full dots) and 2 D (light stars) downstream the WT (a). In (b) the measured values of TI in the wake are scaled by TI_∞.

The retrieved dissipation rates are expected to increase in the wake with increasing upstream turbulence as well. In order to evaluate if our results are comparable to other experiments, we show the measurements in comparison to the best-fit line between turbulence intensity and ε as it was found in Lundquist and Bariteau (2015) [28] (Fig. 6). The Perdigão lidar wake measurements show large scatter with a significant amount of data points at lower values of ε compared to the waked cases from Lundquist and Bariteau (2015). A possible explanation for this can be that the area of highest turbulence of the wake is not always in the RHI plane and the retrieved values of ε are thus underestimating the total turbulence in the rotor plane.

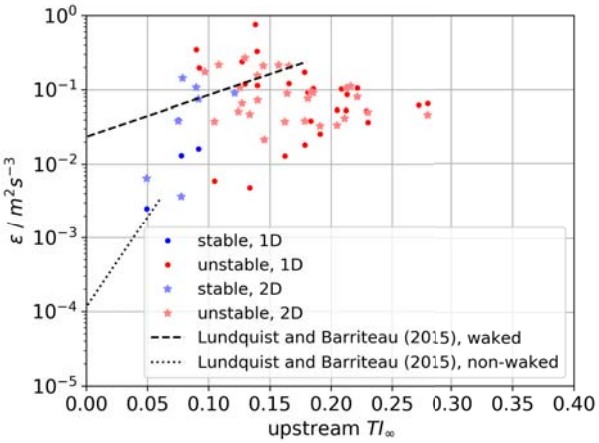

Figure 6. TKE dissipation rate (ε) in the wake as a function of upstream turbulence (TI_∞) for distances of 1 D (full dots) and 2 D downstream the WT (light stars).

5. Conclusion

Within a WT wake, increased levels of turbulence generated by the vortices of the rotor blades can be expected. In this study we quantify this enhancement of atmospheric turbulence up to five rotor diameters downstream through RHI measurements with long-range lidars. We show that the average velocity variance of the flow in the wake is approximately 4 times higher in the wake than upstream in stable atmospheric conditions at 3 D downwind and still 1.5 times higher at 2 D downwind in unstable conditions. We find that an enhancement of turbulence by the wake can be found in conditions with turbulence intensities up to 20%, whereas almost no increase of TI compared to the inflow was observed at TI of 30% or greater. TKE dissipation rate is analyzed as a turbulence parameter which feeds directly into theoretical turbulence models. It is found to be one order of magnitude larger in the wake than upstream in daytime cases and two orders of magnitude in stable cases due to the very weak upstream turbulence. Absolute maximum values of TKE dissipation rate are similar in both regimes.
The study shows that long-range lidars can provide valuable information about wake turbulence and that the use of information of spectral broadening allows to obtain TKE dissipation rate as a comparable parameter of turbulence. The Perdigão 2017 dataset of RHI measurements in the wake contains 80 half-hour periods that were analyzed in this study. In order to discriminate more distinct atmospheric conditions, more data will be needed in future. The experimental setup of RHI scans in Perdigão only allowed a narrow range of wind directions to be analyzed and it is not guaranteed that the wake center is within the plane of observation. In future, the methods described in this study could for example be applied to nacelle-based PPI scans in wind farms, which would allow a much larger database of wake measurements. We also recommend repeating similar measurements in more homogeneous and flat terrain in order to have smaller uncertainties of upstream wind conditions and interaction with the terrain.
The uncertainties of turbulence retrievals with long-range lidars based on common turbulence theory will also be subject to future research as it depends strongly on the integral length scales which are most often not known a priori. In situ instrumentation can help to validate lidar measurements and potentially enable them to be used in operational use for turbulence estimation.

Acknowledgments

We want to thank José Palma, University of Porto and José Caros Matos and the INEGI team for the local organization and tireless work in order to make this experiment a success. We acknowledge all the hard work of the DTU and NCAR staff to provide large parts of the hardware and software infrastructure available at Perdigão. We appreciate the hospitality and help we received from the municipality of Alvaiade Vale do Cobrão and Vila Velha de Rodão throughout the campaign. This work was performed within

projects LIPS and DFWind, both funded by the Federal Ministry of Economy and Energy on the basis of a resolution of the German Bundestag under the contract numbers 0325518 and 0325936A, respectively.
This work was authored [in part] by the National Renewable Energy Laboratory, operated by Alliance for Sustainable Energy, LLC, for the U.S. Department of Energy (DOE) under Contract No. DE-AC36-08GO28308. Funding provided by the U.S. Department of Energy Office of Energy Efficiency and Renewable Energy Wind Energy Technologies Office. The views expressed in the article do not necessarily represent the views of the DOE or the U.S. Government. The U.S. Government retains and the publisher, by accepting the article for publication, acknowledges that the U.S. Government retains a nonexclusive, paid-up, irrevocable, worldwide license to publish or reproduce the published form of this work, or allow others to do so, for U.S. Government purposes.

References

[1] van Kuik G A M *et al.* 2016 *Wind Energy Science* **1** 1–39
[2] Veers P, Dykes *et al.* 2019 *Science* **366** eaau2027
[3] Ainslie J F 1988 *Journal of Wind Engineering and Industrial Aerodynamics* **27** 213–224
[4] Wu Y T and Porté-Agel F 2012 *Energies* **5** 5340–5362
[5] Aitken M L, Kosovic B, Mirocha J D and Lundquist J K 2014 *Journal of Renewable and Sustainable Energy* **6** 033137
[6] Englberger A and Dörnbrack A 2017 *Boundary-Layer Meteorology* **162** 427–449
[7] Englberger A and Dörnbrack A 2018 *Boundary-Layer Meteorology* **166** 423–448
[8] Barthelmie R J, Folkerts L, Ormel F T, Sanderhoff P, Eecen P J, Stobbe O and Nielsen N M 2003 *Journal of Atmospheric and Oceanic Technology* **20** 466–477
[9] Käsler Y, Rahm S, Simmet R and Kühn M 2010 *J. Atmos. Oceanic Technol.* **27** 1529–1532
[10] Iungo G V, Wu Y T and Porté-Agel F 2013 *J. Atmos. Oceanic Technol.* **30** 274–287
[11] Smalikho I N, Banakh V A, Pichugina Y L, Brewer W A, Banta R M, Lundquist J K and Kelley N D 2013 *J. Atmos. Oceanic Technol.* **30** 2554–2570
[12] Aitken M L and Lundquist J K 2014 *Journal of Atmospheric and Oceanic Technology* **31** 1529–1539
[13] Wildmann N, Hofsäß M, Weimer F, Joos A and Bange J 2014 *Advances in Science and Research* **11** 55–61
[14] Herges T G, Maniaci D C, Naughton B T, Mikkelsen T and Sjöholm M 2017 *Journal of Physics: Conference Series* **854** 012021
[15] Mikkelsen T, Sjöholm M, Angelou N and Mann J 2017 *IOP Conference Series: Materials Science and Engineering* **276** 012004
[16] Bodini N, Zardi D and Lundquist J K 2017 *Atmospheric Measurement Techniques* **10** 2881–2896
[17] Wildmann N, Kigle S and Gerz T 2018 *Journal of Physics: Conference Series* **1037** 052006
[18] Menke R, Vasiljević N, Hansen K S, Hahmann A N and Mann J 2018 *Wind Energy Science* **3** 681–691
[19] Barthelmie R, Pryor S, Wildmann N and Menke R 2018 *Journal of Physics: Conference Series* **1037** 052022
[20] Wildmann N, Vasiljevic N and Gerz T 2018 *Atmospheric Measurement Techniques* **11** 3801–3814
[21] Barthelmie R J and Pryor S C 2019 *Atmospheric Measurement Techniques* **12** 3463–3484
[22] Fernando H J S *et al.* 2019 *Bulletin of the American Meteorological Society* **100** 799–819
[23] Wildmann N, Bodini N, Lundquist J K, Bariteau L and Wagner J 2019 *Atmospheric Measurement Techniques* **12** 6401–6423

[24] re3dataorg 2019 Perdigão field experiment URL http://doi.org/10.17616/R31NJMN4
[25] UCAR/NCAR-Earth Observing Laboratory 2019 Ncar/eol quality controlled high-rate isfs surface flux data, geographic coordinate, tilt corrected. version 1.1 URL http://doi.org/10.26023/8X1N-TCT4-P50X
[26] Smalikho I, Köpp F and Rahm S 2005 *Journal of Atmospheric and Oceanic Technology* **22** 1733–1747
[27] Bodini N, Lundquist J K and Newsom R K 2018 *Atmospheric Measurement Techniques* **11** 4291–4308
[28] Lundquist J K and Bariteau L 2015 *Boundary-Layer Meteorology* **154** 229–241